Computational Sciences and Engineering 2(2) (2022) 111-123

University of Guilan

Computational Sciences and Engineering

journal homepage: https://cse.guilan.ac.ir/

Estimation of elastic modulus and Poisson's ratio of concrete containing graphene nanosheets: A focus on nano-filler agglomeration and hydration time

R. Pouyanmehr [a], M. K. Hassanzadeh-Aghdam [b,*], R. Ansari [a]

[a] Faculty of Mechanical Engineering, University of Guilan, Rasht, Iran

[b] Department of Engineering Science, Faculty of Technology and Engineering, East of Guilan, University of Guilan, Rudsar-Vajargah, Iran

ARTICLE INFO

Article history:
Received 24 May 2022
Received in revised form 01 July 2022
Accepted 02 July 2022
Available online 02 July 2022

Keywords:
Concrete
Graphene nanosheet
Elastic property
Hydration
Agglomeration.

ABSTRACT

In the current study, the influences of adding graphene nanosheets (GNSs) on the elastic characteristics of concrete are examined using the Mori-Tanaka micromechanical model. By the use of the base concrete hydration equation, the role of hydration time in the Young's modulus and Poisson ratio of GNS-filled concrete is analyzed. Also, the formation of GNS agglomeration as one of the most major microstructural features of composite materials containing nano-sized particles is considered in the micromechanical simulation. Significant contribution of the hydration time to the elastic properties of GNS-reinforced concrete is confirmed. Generally, the addition of GNSs can help to enhance the concrete elastic modulus and decrease the Poisson's ratio. The results show that well-dispersed GNSs lead to the enhancement of mechanical performance of the concrete, whereas GNS agglomeration causes significant reduction of elastic modulus.

1. Introduction

Concrete is one of the most broadly utilized construction materials in civil engineering all over the world. Concrete is appropriate for the structural purposes since its compressive strength is extremely high. But, ductility, tensile strength and flexural strength of concrete are low which can be known as the main drawbacks of concrete [1,2]. Also, microscale cracks as the chief hidden defects in concrete structures can lead to brittle fractures, shorten the service life, and inferior the durability [3,4]. Numerous efforts have been conducted to prevent the generation of cracks by adding micro-fillers such as glass, carbon, steel or polypropylene fibers into concrete [5-7].

* Corresponding author, Email: Mk.hassanzadeh@gmail.com

https://dx.doi.org/10.22124/cse.2022.22353.1033

Advancements in nanotechnology lead to a variety of nanoscale particles such as carbon nanotubes (CNTs) and graphene nanosheets (GNSs) to be considered as the reinforcements to improve defects of concrete [8-10] and cement matrix composites [11,12]. Graphene consists of a layer of graphite, two dimensional comprising the sp^2-hybridized carbon atoms [13]. It displays exceptional Young's modulus, great fracture strength, extraordinary thermal conductivity and useful functionalities [14-16]. Several attempts exist in the literature about the mechanical properties of graphene-reinforced concrete. For example, Wu et al. [17] accomplished an experimental study on the compressive strength, flexural strength, and tensile strength of concrete containing GNSs at different weight fractions from 0 to 0.08% and the water/cement ratio of 0.5. It was reported when the amount of GNSs amplified from 0.02% to 0.08%, the compressive strength of 28-day specimen enhanced from 46.47 MPa to 55.22 MPa, demonstrating an improvement from 12.84% to 34.08% in comparison with the base concrete specimen. Also, the flexural strength of 28-day GNS-reinforced concrete specimen augmented in a range from 2.77% to 15.60% [17]. Lu and Ouyang [18] examined the influence of GNS additives (0-0.03% by weight of cement) on the mechanical properties of cement mortar and ultra-high strength concrete (UHSC). As compared with unreinforced concrete, adding 0.01 wt.% of GNSs caused a 7.82% enhancement in compressive strength of concrete after 28 days of curing. In another study, Dimov et al. [19] produced an innovative multifunctional concrete reinforced by graphene nanoparticles displaying an extraordinary range of improved properties in comparison with base concrete. An enhancement of up to 146% in the compressive strength and 79.5% in the flexural strength was reported. Also, the thermal efficiency with 88% enhancement in heat capacity of the reinforced concrete was informed [19]. Shamsaei et al. [20] provided an inclusive overview on developments in the production, properties and applications of GNSs in improving the strength and durability of concrete. To date, the majority of investigations has focused on the compressive strength and flexural strength of GNS-reinforced concrete. Limited information has been reported on the elastic characteristics of GNS-reinforced concrete. The Young's modulus and Poisson ratio of concrete containing nano-sized particles are fundamental coefficients needed in structural study for the calculation of the stress and strain values. It is very important as the design becomes on the basis of the elasticity framework. Therefore, it is obvious that further research in this area is necessary.

The micromechanical models can predict the effective properties of cement-based materials from their constituent material properties, amount, reinforcement geometry and interaction between the phases [21-23]. For example, García-Macías et al. [24] offered a micromechanical model to estimate the effective electrical conductivity of CNT-reinforced cement composites. The non-straight shape and non-uniform dispersion of the nano-inclusions were considered. Also, for verifying the correctness of the micromechanical method, some coupons of cement pastes, mortars and concretes

with various amount of CNTs were fabricated and experienced. The experimental measurements were used for the comparisons. It was observed that the micromechanical predictions agreed well with the experiments [24]. In another study, Jang et al. [25] micromechanically evaluated the effects of CNT volume fraction and moisture on the effective electrical conductivity of CNT-reinforced cementitious composites using the Maxwell-Garnett model, the generalized self-consistent model, and the differential scheme. All models could provide good predictions compared to the experimental measurements [25]. By the effective medium micromechanics model, Hassanzadeh-Aghdam et al. [26] determined the thermal conductivities of CNT-reinforced cementitious composites. The predicted values of thermal properties were in very good agreement with experimental data [26]. Also, Wang et al. [27] predicted the elastic modulus of CNT-reinforced cement-based composites with a combination of self-consistent and Mori-Tanaka schemes. They verified the accuracy and efficiency of the micromechanical approach by comparisons with experiments and finite element method [27]. Moreover, Hassanzadeh-Aghdam et al. [28] investigated the influence of adding CNTs on the thermal conductivity of short steel fiber-reinforced concrete by a multi-scale micromechanical approach. The results revealed that the micromechanical predictions and experimental data have high consistency [28].

The aim of this work is to estimate the Young's modulus and Poisson's ratio of concrete containing GNSs by means of a micromechanical model. The influences of formation of GNS agglomeration frequently encountered in real engineering situations, and hydration time in the elastic properties of GNS-reinforced concrete are analyzed. The paper is organized as follows. The basic micromechanical equations of the Mori-Tanaka model are formulated in Section 2. In Section 3, the numerical results for the Young's modulus and Poisson's ratio of GNS-reinforced concrete are presented. Also, some comparisons with experiment are provided in this section. Finally, the main outcomes are summarized in Section 4.

2. Micromechanical approach

The elastic characteristics of the GNS-reinforced concrete are calculated by means of the Mori-Tanaka method which is a well-organized micromechanics-based method [29,30]. From the viewpoint of a composite material, the GNSs as reinforcements are dispersed within the concrete as matrix. Three types of GNS distribution in the concrete in which GNSs are: (1) aligned, (2) uniformly dispersed and (3) agglomerated are considered. The GNP agglomeration significantly reduces the stiffening influence of nano-graphene particles [31,32].

1.1.Aligned GNSs

Based on the Mori-Tanaka model [15,33], the final form of the stiffness tensor of the GNS-reinforced concrete $\mathbf{C}^{NC}$ subjected to the aligned GNS state is given by

$$\mathbf{C}^{NC} = \left(f_m \mathbf{C}_m + \sum_{r=1}^{N} f_r \mathbf{C}_r : \mathbf{A}_r \right) : \left(f_m \, \mathbf{I} + \sum_{r=1}^{N} f_r \, \mathbf{A}_r \right)^{-1} \tag{1}$$

where f_m and f_r are the volume fractions of the concrete and the GNP, respectively, and N indicates the number of reinforcements which may have different characteristics. Also, $\mathbf{I}$ denotes fourth-order identity tensor, and $\mathbf{C}_r$ and $\mathbf{C}_m$ denote fourth-rank stiffness tensor of the nano-graphene reinforcement and concrete matrix, respectively. $\mathbf{A}_r$ specifies the strain-concentration tensor

1.2.Randomly oriented GNSs

The ending form of $\mathbf{C}^{NC}$ subjected to the random distribution of nano-graphene particles is specified as [15]

$$\mathbf{C}^{NC} = \left(f_m \mathbf{C}_m + \sum_{r=1}^{N} f_r \langle \mathbf{C}_r : \mathbf{A}_r(\theta, \varphi) \rangle \right) : \left(f_m \, \mathbf{I} + \sum_{r=1}^{N} f_r \, \langle \mathbf{A}_r(\theta, \varphi) \rangle \right)^{-1} \tag{2}$$

Moreover, derivation of the bulk modulus and shear modulus of the concrete containing randomly oriented GNSs on the basis of the Hill's coefficients of reinforcement and matrix is [15]

$$k^{NC} = k_m + \frac{f_r(\delta_r - 3k_m\alpha_r)}{3(f_m + f_r\alpha_r)}, \tag{3}$$

$$\mu^{NC} = \mu_m + \frac{f_r(\eta_r - 2\mu_m\beta_r)}{2(f_m + f_r\beta_r)},$$

in which

$$\alpha_r = \frac{3k_m + 2n_r - 2l_r}{3n_r}, \tag{4}$$

$$\beta_r = \frac{4\mu_m + 7n_r + 2l_r}{15n_r} + \frac{2\mu_m}{2p_r},$$

$$\delta_r = \frac{3k_m(n_r + 2l_r) + 4(k_r n_r - l_r^2)}{3n_r},$$

$$\eta_r = \frac{2}{15}\left(k_r + 6m_r + 8\mu_m - \frac{l_r^2 + 2\mu_m l_r}{n_r} \right),$$

where subscript m and r represent the matrix and reinforcement, respectively.

1.3.Agglomeration of GNSs

The dispersion of the nano-graphene particles in the concrete may be non-uniform. It means that some local parts have a higher amount of nanoparticles than the average volume fraction in the entire concrete. The concentrated GNS areas are assumed to possess spherical shapes and entitled “agglomeration phase”, while the remaining of concrete comprises a homogenous distribution of GNSs entitled as “effective concrete phase” [15,34]. Too, the nanoparticles are randomly oriented in two phases. For characterizing the GNS agglomeration, two parameters are presented as follows

$$\xi = \frac{V_{agglomer}}{V}, \quad \zeta = \frac{V_r^{agglomer}}{V_r} \tag{5}$$

where V denotes the concrete volume, and $V_{agglomer}$ is the volume of agglomerated part. Moreover, V_r and $V_r^{agglomer}$ are the nanoparticle volume in concrete and in the agglomerated phase, respectively. The nanoparticle volume fractions in the agglomerated phase ($f_r^{agglomer}$) and in the effective concrete phase (f_r^{ecp}) are defined, respectively, by

$$f_r^{agglomer} = \frac{V_r^{agglomer}}{V_{agglomer}} = \frac{\zeta}{\xi} f_r \tag{6}$$

$$f_r^{ecp} = \frac{V_r - V_r^{agglomer}}{V - V_{agglomer}} = \frac{(1-\zeta) f_r}{(1-\xi)}$$

Primary, the elastic characteristics of the agglomerated phase and the concrete phase must be calculated. The bulk modulus and shear modulus of the agglomerated phase can be obtained as

$$k_{agglomer} = k_m + \left[\frac{(\delta_r - 3k_m\alpha_r)\alpha_r\zeta}{3(\xi - f_r\zeta + f_r\zeta\alpha_r)}\right] \tag{7}$$

$$\mu_{agglomer} = \mu_m + \left[\frac{f_r\xi(\eta_r - 2\mu_m\beta_r)}{2(\xi - f_r\zeta + f_r\zeta\beta_r)}\right]$$

In the second step, a like process is accomplished for the prediction of the bulk modulus and shear modulus of concrete phase, as follows

$$k_{emp} = k_m + \left[\frac{f_r(\delta_r - 3k_m\alpha_r)(1-\zeta)}{3(1-\xi - f_r(1-\zeta) + f_r(1-\zeta)\alpha_r)}\right], \tag{8}$$

$$\mu_{emp} = \mu_m + \left[\frac{f_r(1-\zeta)(\eta_r - 2\mu_m\beta_r)}{2(1-\xi - f_r(1-\zeta) + f_r(1-\zeta)\beta_r)}\right]$$

Finally, by consideration of the agglomerated phase as the inclusion and the effective concrete phase as the new matrix, the bulk modulus and shear modulus of GNS-reinforced concrete considering agglomerations are extracted as

$$k = k_{ecp}\left[1 + \frac{\xi\left(\left(k_{agglomer}/k_{ecp}\right) - 1\right)}{1 + \alpha(1-\xi)\left(\left(k_{agglomer}/k_{ecp}\right) - 1\right)}\right], \tag{9}$$

$$\mu = \mu_{ecp}\left[1 + \frac{\xi\left(\left(\mu_{agglomer}/\mu_{ecp}\right) - 1\right)}{1 + \beta(1-\xi)\left(\left(\mu_{agglomer}/\mu_{ecp}\right) - 1\right)}\right]$$

in which

$$\alpha = \frac{3k_{ecp}}{3k_{ecp} + 4\mu_{ecp}}, \beta = \frac{6\left(k_{ecp} + 2\mu_{ecp}\right)}{5\left(3k_{ecp} + 4\mu_{ecp}\right)}. \tag{10}$$

3. Results and discussion

To show the correctness of the micromechanics model, a comparison is made among the calculations and experiments available in the literature for the elastic modulus of GNS-reinforced concrete [19]. The Young's modulus and Poisson's ratio of the base concrete are 32.2 GPa and 0.2, respectively, which its Hill's parameters are determinable. Hill's coefficients of the GNS equal to $2k$=1700 GPa, l=6.8 GPa, n=102000 GPa, $2m$=738 GPa and $2p$=204000 GPa, respectively. Also, the water-cement ratio (W/C) is 0.57. According to Ref. [19], a uniform dispersion of the graphene nanoparticles has been reported. The Young's modulus determined using the micromechanical model and experimental measurements [19] are shown in Fig. 1. The difference between the two sets of results is small, and close agreement between the micromechanical model and experiment [19] can be found. It is clear that the presence of the graphene nanoparticles affects the mechanical properties of concrete system. The elastic modulus is enhanced as the amount of graphene nanoparticle increases.

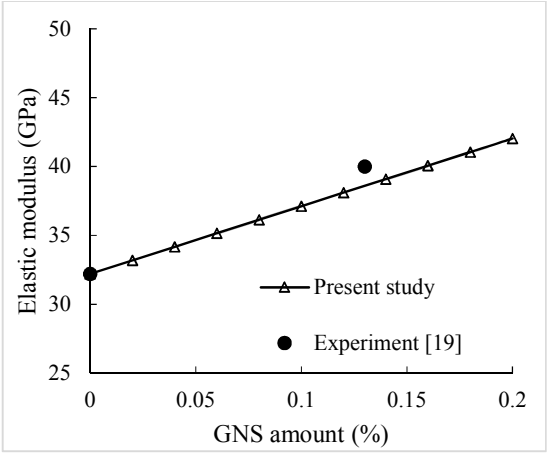

Fig. 1. Comparison of the elastic modulus of GNS-reinforced concrete predicted by the proposed micromechanical model and experimental data [19]

The numerical magnitudes of the Young's modulus and Poisson's ratio of GNS-reinforced concrete are obtained. In the present study, the hydration time is investigated using the base concrete hydration equation. As discussed in Ref. [35], the concrete hydration equation has the general following form

$$K = K_{\infty} \pm bt^{-p} \tag{11}$$

where K denotes the hydration criterion examined, and K_{∞} and b are constant parameters. Also, t stands for the hydration time stated in days, and p is the hydration number, which is a constant for a concrete system. Based on the hydration equation, the elastic modulus and Poisson's ratio of

concrete (Portland cement I, Cement 340 kg/m^3, W/C= 0.5, Grading B32 consistent with DIN 1025) as a function of time can be given, respectively, by [35]

$$E_C = 51.1983 - 31.1522 \times t^{-0.394}, \quad (12)$$

$$v_C = 0.3515 - 0.2726 \times t^{-0.394}$$

Fig. 2 a and b show the Young's modulus and Poisson's ratio of GNS-filled concrete, respectively, versus time. In this figure both types of GNS dispersion into the concrete: (i) uniformly dispersed and (ii) agglomerated state are analyzed. The GNS volume fraction is assumed to be 5%. Also, the elastic properties of the base concrete are included in Fig. 2. The results indicate that there is strong effect of GNSs on the elastic properties of concrete. Fig. 2a displays that the addition of GNSs into the concrete results in an improvement of Young's modulus, since the Young's modulus of GNSs is greater than that of the base concrete. Furthermore, the elastic modulus of concrete having a uniform dispersion of GNSs is greater than that of concrete with GNS agglomeration. In fact, locally agglomerated region acts as the stress concentration area which is a defect in the GNS-reinforced concrete. Thus, one critical factor which should be satisfied for obtaining high mechanical performance in GNP-reinforced concrete is uniform distribution of the nano-graphene particles into the cement-based materials. By increasing time, the elastic modulus of GNS-reinforced concrete sharply increases, followed by an expected slight increase. Poisson's ratio of concrete decreases with adding the GNSs as depicted in Fig. 2b. However, the GNS agglomeration can slightly increase the Poisson's ratio of the reinforced concrete. It is concluded from this figure that with the increase of time, there is an asymptotically rise for the Poisson's ratio of GNS-reinforced concrete.

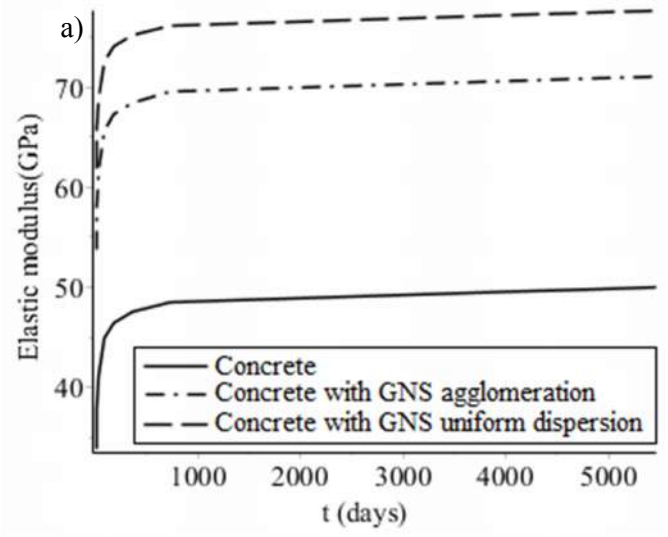

b)

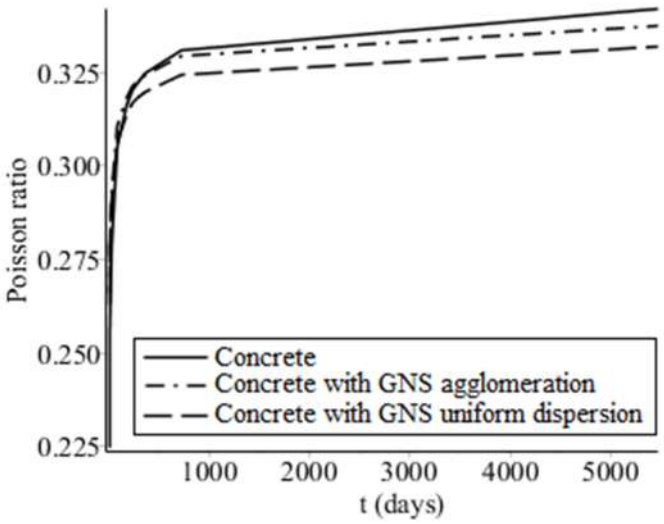

Fig. 2. Variation of (a) elastic modulus and (b) Poisson's ratio of GNS-reinforced concrete as a function of time

The variation of Young's modulus and Poisson's ratio of GNS-filled concrete with GNS volume fraction is shown in Fig. 3 a and b, respectively. The results are determined for two conditions: (i) uniform dispersion and (ii) agglomerated state of GNSs. Micromechanical results of Fig. 3a have demonstrated that increasing the volume fraction of uniformly distributed GNSs can effectively enhance the elastic modulus of concrete, confirming GNS as an exceptional candidate for utilizing as the nano-filler in cement matrix materials. The agglomeration of nanosheets in the concrete with higher concentrations of GNS can be incorporated as the key effective factor in decreasing the mechanical performance. It is clarified from Fig. 3b that Poisson's ratio of the reinforced concrete can be decreased with increasing GNS amount.

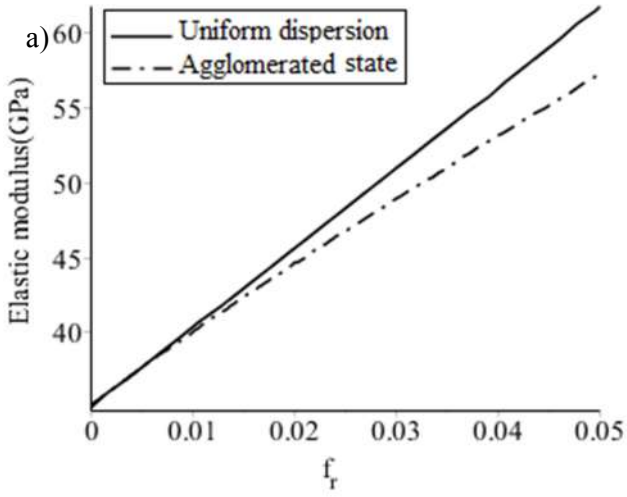

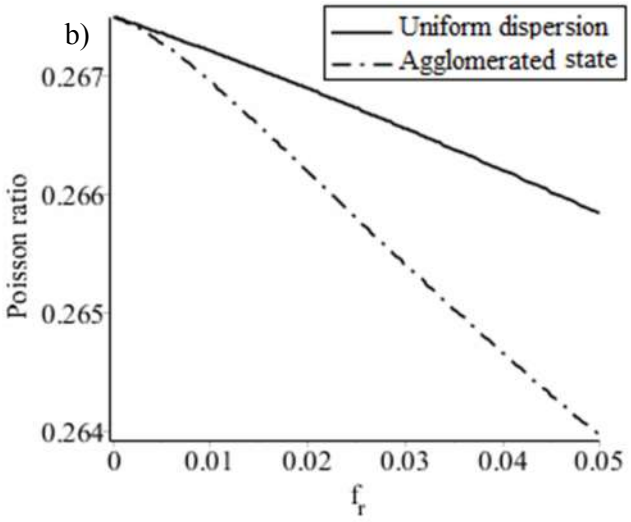

Fig. 3. Variation of (a) elastic modulus and (b) Poisson's ratio of GNS-reinforced concrete as a function of GNS amount

Fig. 4a illustrates the relation among the elastic modulus of GNS-reinforced concrete and agglomeration factors. The elastic modulus enhances with rising the value of ξ and takes the maximum value once the GNSs are homogenously distributed in the concrete ($\xi = \zeta$). The relation between the Poisson's ratio of GNS-reinforced concrete and agglomeration parameters is depicted in Fig. 4b. A nonlinear trend in Poisson's ratio behavior can be observed.

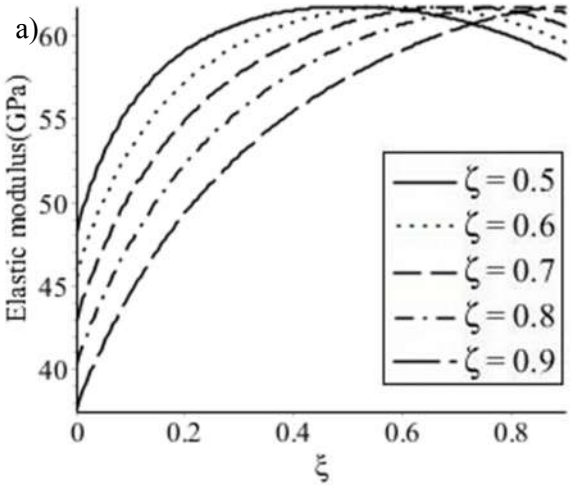

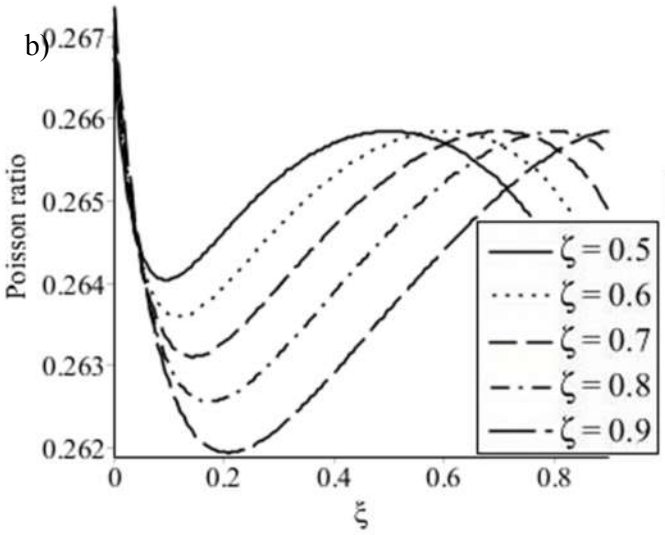

Fig. 4. Effect of agglomeration parameters on the (a) elastic modulus and (b) Poisson's ratio of GNS-reinforced concrete.

Fig. 5a displays the influence of nanoparticle agglomeration on GNS-filled concrete elastic modulus with ξ=1 for the different GNS amounts. The effective elastic modulus is rapidly decreased with reducing the agglomeration factor ζ. Once ζ=1, adding the GNSs into the concrete highly improves the effective elastic modulus. The influence of agglomeration parameter on the GNS-reinforced concrete Poisson's ratio with ξ=1 for diverse GNS amounts is revealed in Fig. 5b. The Poisson's ratio increases with the decrease of agglomeration parameter ζ.

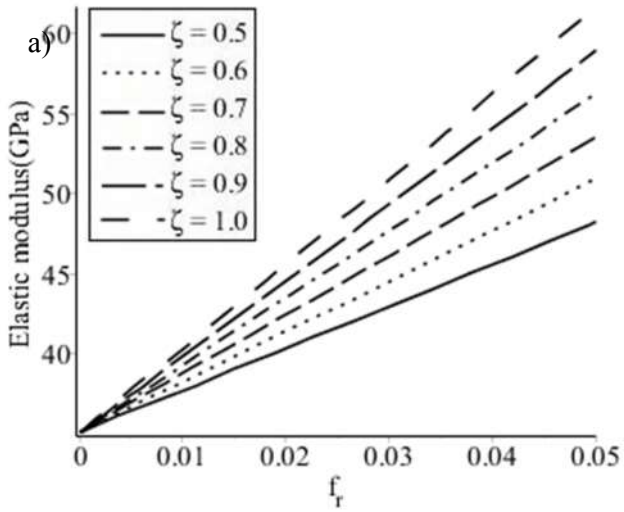

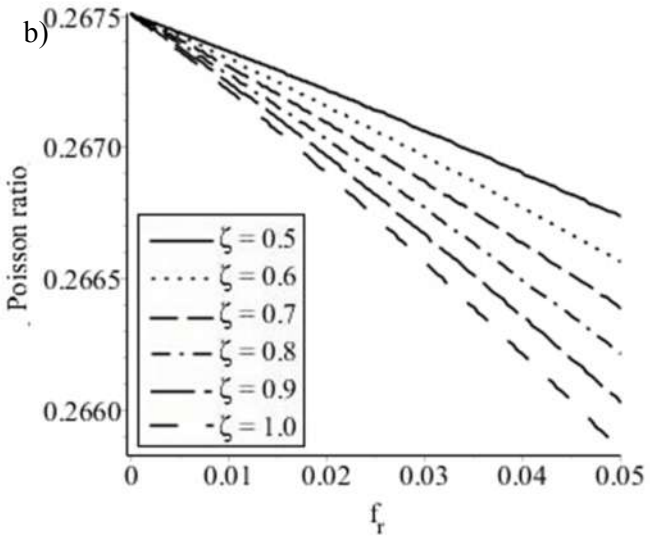

Fig. 5. Effect of agglomeration with ξ=1 on the (a) elastic modulus and (b) Poisson's ratio of GNS-reinforced concrete for different GNS volume fractions.

4. Conclusions

In this work, a micromechanical model was proposed to predict the elastic modulus and Poisson's ratio of concrete reinforced by GNSs. The effect of hydration time in the elastic properties of GNS-reinforced concrete was analyzed using the base concrete hydration equation. It was found that adding the GNSs with a uniform dispersion results in a significant enhancement of mechanical performance of the reinforced concrete. But, forming the nano-graphene agglomeration decreased the reinforced concrete Young's modulus. The Poisson's ratio of the concrete reinforced by uniformly dispersed GNSs was lower than that of the concrete containing agglomerated GNSs. The results indicated that as the time increases, the elastic modulus of GNS-reinforced concrete sharply increases and then, its value saturates. Also, comparative studies revealed that the calculations of the micromechanics method were in good agreement with the experiments.

References

1. Radnić, J., Markić, R., Glibić, M., Ćubela, D., & Grgić, N. (2016). Experimental testing of concrete beams with different levels of prestressing. Proceedings of the Institution of Mechanical Engineers, Part L: Journal of Materials: Design and Applications, 230(3), 760-779.
2. Moosaei, H. R., Zareei, A. R., Salemi, N. (2022). Elevated Temperature Performance of Concrete Reinforced with Steel, Glass, and Polypropylene Fibers and Fire-proofed with Coating, International Journal of Engineering, 35(05), 917-930.
3. Jefferson, A. D. (2002). Local plastic surfaces for cracking and crushing in concrete. Proceedings of the Institution of Mechanical Engineers, Part L: Journal of Materials: Design and Applications, 216(4), 257-266.
4. Jefferson, A. D. (2002). Local plastic surfaces for cracking and crushing in concrete. Proceedings of the Institution of Mechanical Engineers, Part L: Journal of Materials: Design and Applications, 216(4), 257-266.
5. Sivaraja, M., Velmani, N., & Pillai, M. S. (2010). Study on durability of natural fibre concrete composites using mechanical strength and microstructural properties. Bulletin of Materials Science, 33(6), 719-729.
6. Akcay, B. (2012). Experimental investigation on uniaxial tensile strength of hybrid fibre concrete. Composites Part B: Engineering, 43(2), 766-778.
7. Schneider, K., Michel, A., Liebscher, M., Terreri, L., Hempel, S., & Mechtcherine, V. (2019). Mineral-impregnated carbon fibre reinforcement for high temperature resistance of thin-walled concrete structures. Cement and Concrete Composites, 97, 68-77.
8. Pradhan, S. C. (2012). Buckling analysis and small scale effect of biaxially compressed graphene sheets using non-local elasticity theory. Sadhana, 37(4), 461-480.
9. Lee, J. H., & Lee, B. G. (2017). Experimental and mechanical analysis of cement–nanotube nanocomposites. Bulletin of Materials Science, 40(4), 819-829.
10. Wang, Z., Yu, J., Li, G., Zhang, M., & Leung, C. K. (2019). Corrosion behavior of steel rebar embedded in hybrid CNTs-OH/polyvinyl alcohol modified concrete under accelerated chloride attack. Cement and Concrete Composites, 100, 120-129.
11. Chu, H. Y., Jiang, J. Y., Sun, W., & Zhang, M. (2017). Effects of graphene sulfonate nanosheets on mechanical and thermal properties of sacrificial concrete during high temperature exposure. Cement and Concrete Composites, 82, 252-264.
12. Liu, J., Li, Q., & Xu, S. (2019). Reinforcing Mechanism of Graphene and Graphene Oxide Sheets on Cement-Based Materials. Journal of Materials in Civil Engineering, 31(4), 04019014.
13. Ahmad, H., Fan, M., & Hui, D. (2018). Graphene oxide incorporated functional materials: A review. Composites Part B: Engineering, 145, 270-280.
14. Luo, H., Dong, J., Xu, X., Wang, J., Yang, Z., & Wan, Y. (2018). Exploring excellent dispersion of graphene nanosheets in three-dimensional bacterial cellulose for ultra-strong nanocomposite hydrogels. Composites Part A: Applied Science and Manufacturing, 109, 290-297.
15. Ji, X. Y., Cao, Y. P., & Feng, X. Q. (2010). Micromechanics prediction of the effective elastic moduli of graphene sheet-reinforced polymer nanocomposites. Modelling and Simulation in Materials Science and Engineering, 18(4), 045005.
16. de Mendonça, J. P. A., Silva, J. P. C., & Sato, F. (2019). High-Frequency Oscillator Based on Nano Graphene. Brazilian Journal of Physics, 49(4), 488-493.
17. Wu, Y. Y., Que, L., Cui, Z., & Lambert, P. (2019). Physical properties of concrete containing graphene oxide nanosheets. Materials, 12(10), 1707.
18. Lu, L., & Ouyang, D. (2017). Properties of cement mortar and ultra-high strength concrete incorporating graphene oxide nanosheets. Nanomaterials, 7(7), 187.
19. Dimov, D., Amit, I., Gorrie, O., Barnes, M. D., Townsend, N. J., Neves, A. I., ... & Craciun, M. F. (2018). Ultrahigh performance nanoengineered graphene–concrete composites for multifunctional applications. Advanced Functional Materials, 28(23), 1705183.
20. Shamsaei, E., de Souza, F. B., Yao, X., Benhelal, E., Akbari, A., & Duan, W. (2018). Graphene-based nanosheets for stronger and more durable concrete: A review. Construction and Building Materials, 183, 642-660.
21. Hlobil, M., Šmilauer, V., & Chanvillard, G. (2016). Micromechanical multiscale fracture model for compressive strength of blended cement pastes. Cement and Concrete Research, 83, 188-202.

22. Hernández, M. G., Anaya, J. J., Ullate, L. G., & Ibañez, A. (2006). Formulation of a new micromechanic model of three phases for ultrasonic characterization of cement-based materials. Cement and Concrete Research, 36(4), 609-616.
23. Tatar, J., Taylor, C. R., & Hamilton, H. R. (2019). A multiscale micromechanical model of adhesive interphase between cement paste and epoxy supported by nanomechanical evidence. Composites Part B: Engineering, 172, 679-689.
24. García-Macías, E., D'Alessandro, A., Castro-Triguero, R., Pérez-Mira, D., & Ubertini, F. (2017). Micromechanics modeling of the electrical conductivity of carbon nanotube cement-matrix composites. Composites Part B: Engineering, 108, 451-469.
25. Jang, S. H., Hochstein, D. P., Kawashima, S., & Yin, H. (2017). Experiments and micromechanical modeling of electrical conductivity of carbon nanotube/cement composites with moisture. Cement and Concrete Composites, 77, 49-59.
26. Hassanzadeh-Aghdam, M. K., Ansari, R., Mahmoodi, M. J., Darvizeh, A., & Hajati-Modaraei, A. (2018). A comprehensive study on thermal conductivities of wavy carbon nanotube-reinforced cementitious nanocomposites. Cement and Concrete Composites, 90, 108-118.
27. Wang, J. F., Zhang, L. W., & Liew, K. M. (2017). Multiscale simulation of mechanical properties and microstructure of CNT-reinforced cement-based composites. Computer Methods in Applied Mechanics and Engineering, 319, 393-413.
28. Hassanzadeh-Aghdam, M. K., Mahmoodi, M. J., & Safi, M. (2019). Effect of adding carbon nanotubes on the thermal conductivity of steel fiber-reinforced concrete. Composites Part B: Engineering, 106972.
29. Hasanzadeh, M., Ansari, R., & Hassanzadeh-Aghdam, M. K. (2019). Evaluation of effective properties of piezoelectric hybrid composites containing carbon nanotubes. Mechanics of Materials, 129, 63-79.
30. Safi, M., Hassanzadeh-Aghdam, M. K., & Mahmoodi, M. J. (2019). Effects of nano-sized ceramic particles on the coefficients of thermal expansion of short SiC fiber-aluminum hybrid composites. Journal of Alloys and Compounds, 803, 554-564.
31. Atif, R., & Inam, F. (2016). Reasons and remedies for the agglomeration of multilayered graphene and carbon nanotubes in polymers. Beilstein journal of nanotechnology, 7(1), 1174-1196.
32. Li, Z., Chu, J., Yang, C., Hao, S., Bissett, M. A., Kinloch, I. A., & Young, R. J. (2018). Effect of functional groups on the agglomeration of graphene in nanocomposites. Composites Science and Technology, 163, 116-122.
33. Mori, T., & Tanaka, K. (1973). Average stress in matrix and average elastic energy of materials with misfitting inclusions. Acta metallurgica, 21(5), 571-574.
34. Dastgerdi, J. N., Marquis, G., & Salimi, M. (2013). The effect of nanotubes waviness on mechanical properties of CNT/SMP composites. Composites Science and Technology, 86, 164-169.
35. Sideris, K. K., Manita, P., & Sideris, K. (2004). Estimation of ultimate modulus of elasticity and Poisson ratio of normal concrete. Cement and Concrete Composites, 26(6), 623-631.